

# DIELECTRIC MEASUREMENTS FOR LOW-LOSS MATERIALS USING TRANSMISSION PHASE-SHIFT METHOD

K. Y. You<sup>a\*</sup>, Y. S. Lee<sup>b</sup>, L. Zahid<sup>b</sup>, M. F. A. Malek<sup>c</sup>, K. Y. Lee<sup>d</sup>, E. M. Cheng<sup>e</sup>, N. H. H. Khamis<sup>a</sup>

<sup>a</sup>Communication Engineering Department, Faculty of Electrical Engineering, Universiti Teknologi Malaysia, 81310 UTM Johor Bahru, Malaysia

<sup>b</sup>School of Computer and Communication engineering, Universiti Perlis Malaysia, 02600 Perlis, Malaysia

<sup>c</sup>School of Electrical Systems Engineering, Universiti Malaysia Perlis, 02600 Perlis, Malaysia

<sup>d</sup>Department of Electrical and Electronic Engineering, Faculty of Engineering and Science, Universiti Tunku Abdul Rahman, 46200 Selangor, Malaysia

<sup>e</sup>School of Mechatronic, Universiti Malaysia Perlis, 02600 Perlis, Malaysia

## Article history

Received

2 July 2014

Received in revised form

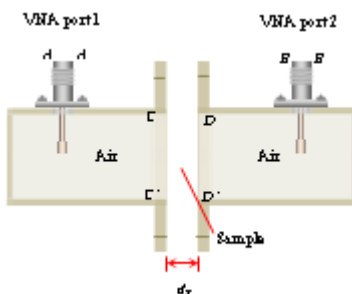
19 July 2015

Accepted

25 November 2014

\*Corresponding author  
kyyou@fke.utm.my

## Graphical abstract



## Abstract

This paper presents a calculation of the dielectric properties of low-loss materials using the transmission phase-shift method. This method can provide calibration-independent and position-insensitive features, and it was verified experimentally by measuring several well-known samples using X-band rectangular waveguides.

**Keywords:** Rectangular waveguides, dielectric constant, loss factor, transmission phase-shift, sample thickness

## Abstrak

Kertas kerja ini membentangkan pengiraan sifat dielektrik untuk bahan lengai dengan menggunakan kaedah penghantaran cara anjakan-fasa. Kaedah ini bebas daripada penentuan dan tidak bersandar kepada kedudukan bahan yang diletakkan dalam pandu gelombang. Kaedah ini telah disahkan secara eksperimen dengan mengukur beberapa sampel yang terkenal dengan menggunakan X-band pandu gelombang yang berbentuk segi empat.

**Kata kunci:** Pandu gelombang berbentuk segi empat, pemalar dielektrik, faktor susutan, penghantaran cara anjakan-fasa, ketebalan sampel

© 2015 Penerbit UTM Press. All rights reserved

### 1.0 INTRODUCTION

Conventionally, the relative permittivity,  $\epsilon_r$ , and relative permeability,  $\mu_r$ , of a sample filled in a waveguide are obtained by measuring and converting the complex reflection coefficient,  $S_{11}$ , and the complex transmission coefficient,  $S_{21}$ , by using Nicholson-Ross-Weir (NRW)<sup>1-2</sup> or improved NRW routines.<sup>3-5, 8-9</sup> Some methods for matching the propagation boundaries have been proposed that require the measurement of only one of these properties for non-magnetic, thin samples. However, the phase of the measured  $S_{11}$  and  $S_{21}$  depends on the position of the calibration reference plane and on consistent positioning of the sample in the waveguide. The uncertainty of phase shift in the measured  $S_{11}$  and  $S_{21}$  can result in an incorrect prediction of the permittivity of the sample. Thus, normally, the calibration plane is referred to the air-material interface, and the thickness of the sample is essentially constant. Another problem that can occur in the broadband measurements of  $S_{11}$  and  $S_{21}$  is phase-shift ambiguity. Although, the thickness,  $d$ , of the material should be less than 25% of the operational wavelength, i.e.,  $\lambda/4$ , this condition does not guarantee the elimination of phase ambiguity over a range of operational frequencies. In earlier work, the ambiguity problem was solved by using group-delay analysis<sup>1-2</sup> and iterative/non-iterative methods.<sup>3-4</sup> Recently, several new calibration-independent and material position-invariant techniques<sup>10-12</sup> have been used to reduce the complexity of the de-embedding procedures and to provide techniques that are applicable for different thicknesses of samples when using this measurement method. In their calibration procedures, most of these new techniques require obtaining the solution of a matrix or the solution of matrix determinants.<sup>10, 12</sup> In addition, the prediction of the tangential loss,  $\tan \delta$ , for low-loss samples from measured  $S_{11}$  and  $S_{21}$  lacks sufficient resolution.<sup>9</sup> It is well known that resonance measurement techniques are good choices for determining low  $\tan \delta$  values, but such techniques cannot be used for the measurement of swept frequency. This paper presents the simple calculation of dielectric properties based on the difference in the phase shifts for the measured  $S_{21}$  between the air and the sample, which was capable of handling the above issues. In this work, formulations were explicitly expressed for the dielectric constant,  $\epsilon_r'$ , and the loss factor,  $\epsilon_r''$ . This method does not involve having to make an initial estimate of the anticipated value or solving a matrix. However, to make these calculations, the samples were assumed to be homogeneous, isotropic, and non-magnetic isotropic, and non-magnetic ( $\mu_r=1$ ).

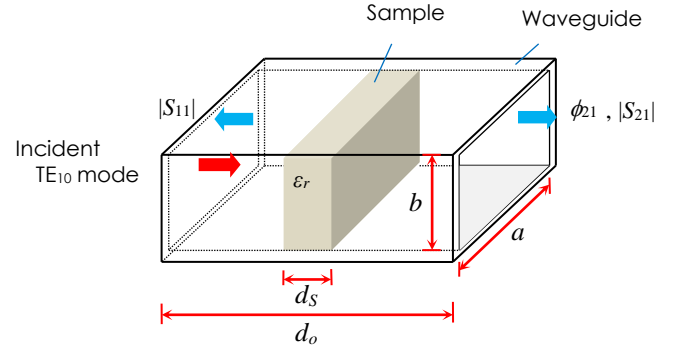


Figure 1 Rectangular waveguide with a sample of  $d_s$  thickness.

### 2.0 PRINCIPLE OF THE TRANSMISSION LINE

The transmission ( $S_{21}$ ) /reflection ( $S_{11}$ ) measurement using rectangular waveguide is shown in Fig. 1, in which a homogeneous and isotropic sample slab with thickness  $d_s$  is partly placed in the rectangular waveguide.

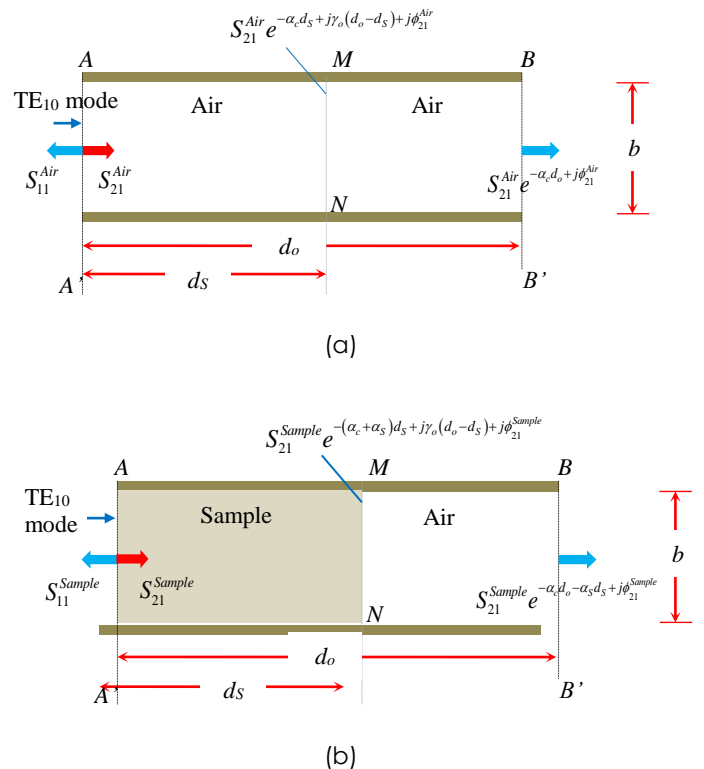


Figure 2 (a) Model of a transmission line: propagating TE<sub>10</sub> wave, attenuation and phase shifted inside waveguide. (b) A sample of  $d_s$  thickness filled in waveguide holder with length of  $d_s$ .

For the TE<sub>10</sub> propagation mode, the relationship between the transmission phase shift,  $\phi_{21}^{Air}$  (in radians), and the propagation constant,  $\gamma_o$ , in an air-filled rectangular waveguide with the length of  $d_o$ , can be represented by a model (cross-sectional view of rectangular waveguide) as shown in Fig. 2 (a). The shifted phase,  $\phi_{21}^{Air}$  (at reference BB'), can be embedded to surface, MN, which has a length of  $d_s$  from AA':<sup>2</sup>

$$\begin{aligned} & -\alpha_c d_s + j \left[ \phi_{21}^{Air} + \gamma_o (d_o - d_s) \right] \\ & = -j \gamma_o d_s \\ & = -j d_s \sqrt{k_o^2 - \left( \frac{\pi}{a} \right)^2} \end{aligned} \quad (1)$$

where  $\alpha_c$  is the conductor attenuation constant (in nepers/meter). When the waveguide is filled with a sample that has a thickness of  $d_s$  (in meter), as shown in Fig. 2 (b), the phase shift,  $\phi_{21}^{Sample}$  (in radians) from reference surface, AA' to surface MN, will be changed based on its new propagation constant,  $\gamma_s$ , as shown:

$$\begin{aligned} & -(\alpha_c + \alpha_s) d_s + j \left[ \phi_{21}^{Sample} + \gamma_o (d_o - d_s) \right] \\ & = -j \gamma_s d_s \\ & = -j d_s \sqrt{k_o^2 (\epsilon_r' - j \epsilon_r'') - \left( \frac{\pi}{a} \right)^2} \end{aligned} \quad (2)$$

where  $k_o = 2\pi f/c$  is the propagation constant of free space ( $c = 2.99792458 \text{ ms}^{-1}$ );  $a$  (in meter) are the width of the aperture of the waveguide, respectively (X-band:  $a = 0.02286 \text{ m}$ ,  $b = 0.01016 \text{ m}$ );  $\epsilon_r = \epsilon_r' - j \epsilon_r''$  and  $\alpha_s$  (in nepers/meter) are the relative permittivity and the dielectric attenuation constant for the sample, respectively. The  $\alpha_s$  is calculated from:

$$\alpha_s \approx -1.15129254 \left[ \begin{array}{l} \log_{10} \left( \left| S_{11}^{Sample} \right|^2 + \left| S_{21}^{Sample} \right|^2 \right) \\ - \log_{10} \left( \left| S_{11}^{Air} \right|^2 + \left| S_{21}^{Air} \right|^2 \right) \end{array} \right] \quad (3)$$

where  $|S_{11}^{Sample}|$  and  $|S_{21}^{Sample}|$  are the measured linear magnitudes of the reflection coefficient and the transmission coefficient for the sample, respectively.

The difference between the phase shift of (1) and the phase shift of (2) can be written as:

$$\alpha_s d_s + j \left( \phi_{21}^{Air} - \phi_{21}^{Sample} \right) = -j (\gamma_o - \gamma_s) d_s \quad (4)$$

From (4), the dielectric constant,  $\epsilon_r'$  and the loss factor,  $\epsilon_r''$  of the sample can be expressed as:

$$\epsilon_r' = \frac{1}{k_o^2} \left\{ \left( \sqrt{k_o^2 - \left( \frac{\pi}{a} \right)^2} + \frac{\phi_{21}^{Air} - \phi_{21}^{Sample}}{d_s} \right)^2 + \left( \frac{\pi}{a} \right)^2 - \alpha_s^2 \right\} \quad (5)$$

$$\epsilon_r'' = \frac{2\alpha_s}{k_o^2} \left( \sqrt{k_o^2 - \left( \frac{\pi}{a} \right)^2} + \frac{\phi_{21}^{Air} - \phi_{21}^{Sample}}{d_s} \right) \quad (6)$$

However, (5) and (6) are only applicable for the ideal case. Normally, the dielectric constant,  $\epsilon_r'$  of the material can be accurately predicted using (5) and (6) at the center operating frequency,  $f_{center}$  of the waveguide (X-band:  $f_{center} = 10.3 \text{ GHz}$ ). For broadband measurements, (5) and (6) should be modified by multiplying (5) with A term as:

$$\epsilon_r' = \frac{A}{k_o^2} \left\{ \left( \sqrt{k_o^2 - \left( \frac{\pi}{a} \right)^2} + \frac{\phi_{21}^{Air} - \phi_{21}^{Sample}}{d_s} \right)^2 + \left( \frac{\pi}{a} \right)^2 - \alpha_s^2 \right\} \quad (7)$$

$$\epsilon_r'' = \frac{2A\alpha_s}{k_o^2} \left( \sqrt{k_o^2 - \left( \frac{\pi}{a} \right)^2} + \frac{\phi_{21}^{Air} - \phi_{21}^{Sample}}{d_s} \right) \quad (8)$$

where

$$A = \left( \frac{f}{f_{center}} \right)^\beta$$

Symbol  $f$  is the operating frequencies. The  $\beta$  is a constant value depended on the model and the quality of the rectangular waveguide. In this study, the  $\beta$  is equal to 0.3. In fact, the A coefficient is used to correct the imperfection of propagation wave (such as VSWR effects) in the rectangular waveguide at lower or upper limit of the operating frequencies.

### 3.0 MEASUREMENT SETUP

The linear magnitude,  $|S_{11}|$ ,  $|S_{21}|$ , and the phase shift,  $\phi_{21}$ , for air and the sample were measured with an Agilent E5071C vector network analyzer (VNA) using two X-band rectangular waveguides (Flann 16094-SF40 Model waveguide adaptors) from 8.2 GHz to 12.4 GHz. For the conventional measurement techniques (such as NWR method or Keysight 85071E software), the thru-reflect-line (TRL) calibration should be done on the surface of  $CC'$  and  $DD'$  which are the exact surface between the samples and the waveguide as shown in Fig. 3 (a). Thus, the position of the sample in the waveguide is dependent on the calibration plane. However, in this study, either open-short-load-thru (OSLT) or TRL calibration is required. The OSLT calibration is normally applied to VNA-ports on  $AA'$  and  $BB'$  planes, respectively. If there is existing waveguide calibration tool kits, thus, the calibration process can be performed on plane  $CC'$  and  $DD'$ , respectively. The sample with thickness  $d_s$  is permitted to place in any position in the rectangular waveguide, which does not affect the accuracy of the measurement.

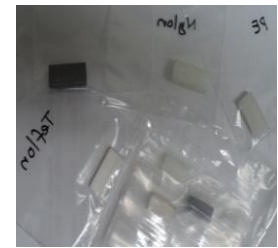
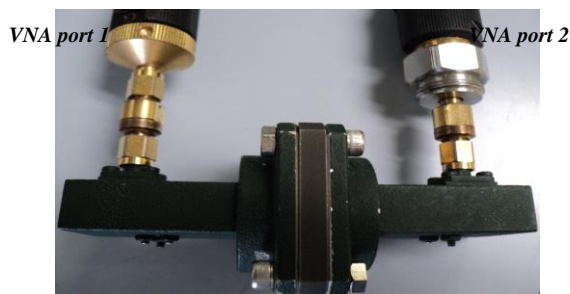
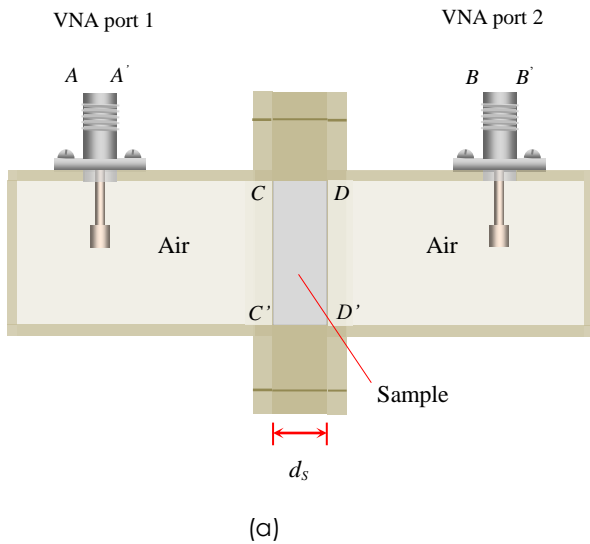


**Figure 3** (a) Cross-sectional view of experimental setup. (b) Actual measurement setup. (c) Customized sample holders. (d) Well known dielectric samples in plastic cover.

The actual measurement setup is shown in Fig. 3 (b). The nylon 6 ( $d = 5$  mm), Teflon ( $d = 5$  mm), PVC ( $d = 5$  mm), and FR4 ( $d = 4.74$  mm) samples, respectively, were placed in the waveguides and measured for

**Table 1** Absolute errors due to  $\pm 0.1$  radian deviation in  $(\phi_{21}^{Air} - \phi_{21}^{Sample})$

$d_s$ (m)	$\pm \Delta \epsilon_r'$		$\pm (\Delta \epsilon_r'' / \Delta \epsilon_r')$	
	10 GHz	15 GHz	10 GHz	15 GHz
0.01	0.07	0.05	0.015	0.010
0.005	0.15	0.10	0.015	0.010
0.001	0.80	0.56	0.014	0.009

**Table 2** Dielectric constant and loss tangents

Material	$\epsilon_r'$		This Study 10.3 GHz
	1-10 GHz	12.4 GHz	
Teflon	2.2 – 1.9 <sup>15</sup>	2.11 $\pm$ 0.05 <sup>16</sup>	2.07
Nylon	3.5 – 2.5 <sup>15</sup>	–	2.99
PVC	2.6 – 2.5 <sup>11</sup>	2.88 $\pm$ 0.04 <sup>16</sup>	2.76
FR4	4.2 – 3.9 <sup>17</sup>	–	3.82

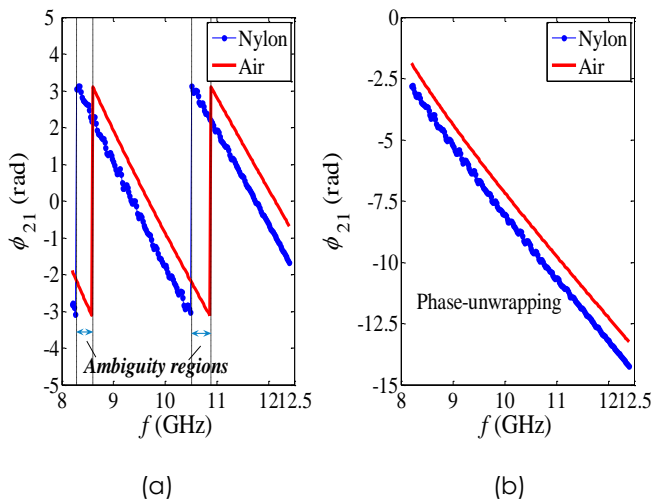
  

Material	Loss tangent, $\tan \delta$		This Study 10.3 GHz
	1-10 GHz	12.4 GHz	
Teflon	0.0001 – 0.0002 <sup>15</sup>	–	0.0002
Nylon	0.01 – 0.05 <sup>15</sup>	–	0.022
PVC	0.0016 – 0.0003 <sup>11</sup>	0.0079 <sup>16</sup>	0.007
FR4	0.018 – 0.022 <sup>17</sup>	–	0.056

validation. The dimensions of the samples were precisely machined by using a computer numerical control (CNC) cutter in order to fit the sample into the waveguide holder.

#### 4.0 RESULTS AND ANALYSIS

The uncalibrated measurements took into account the total propagation wavelength ( $>\lambda/4$ ) within the length of the waveguide and the length of the sample, which caused phase-ambiguity regions due to the variation of phase shift between air and the sample over a given frequency range, as shown in Fig. 4(a). Thus, the predicted values of  $\epsilon_r'$  and  $\epsilon_r''$  would be incorrect. In this study, the phase ambiguity was solved by using MATLAB's 'unwrap' command<sup>13</sup>, as shown in Fig. 4(b).



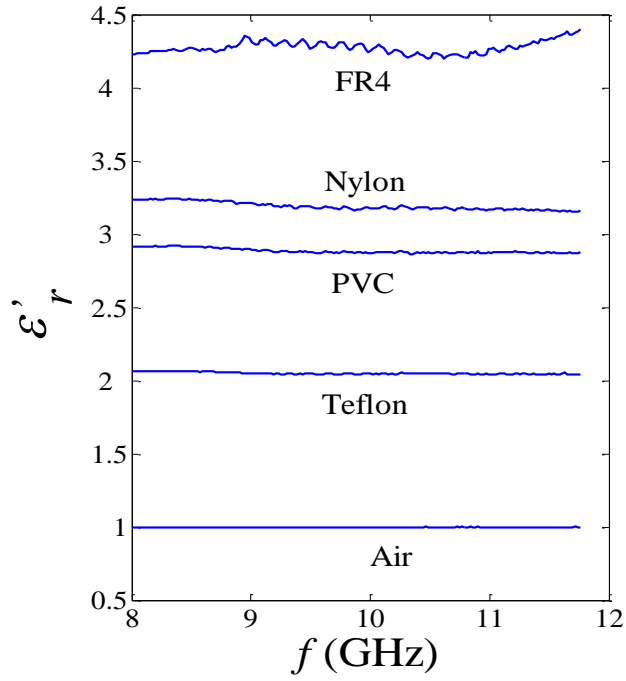
**Figure 4** (a) Phase ambiguity in uncalibrated measurements between air and nylon; (b) Phase ambiguity solved by using the phase-unwrapping method

As known that the conventional NRW method requires sample thickness must be less than  $\lambda/4$  in order to avoid phase ambiguity in the dielectric measurements. However, for this study method, the minimum thickness of the sample was limited to  $\lambda/8$ . The uncertainty measurement is high for a thin sample due to the decreasing of the sensitivity for the transmitted wave through the sample, especially for

transmitted waves that have longer wavelengths. For instance, a deviation of  $\pm 0.1$  radian in the measurement of  $(\phi_{21}^{Air} - \phi_{21}^{Sample})$  for nylon, may cause different absolute errors, i.e.,  $\Delta \epsilon_r'$  and  $\Delta \epsilon_r''$ , in the prediction of the dielectric properties depending on the thickness,  $d_s$ , of the nylon, as shown in Table I. The  $\epsilon_r'$  results at 10.3 GHz using this study method were in good agreement with the measurements obtained from literatures,<sup>15-17</sup> as tabulated in Table II.

Fig. 5 (a) and (b) show the measured dielectric constant,  $\epsilon_r'$  and loss tangent,  $\tan \delta (= \epsilon_r''/\epsilon_r')$ , for four types of low loss samples using NRW method (See Appendix) from 8.2 GHz to 11.75 GHz. The ambiguity phase exists when the operating frequency exceeds 11.75 GHz for the 0.5 mm thickness of the samples. The dielectric constant,  $\epsilon_r'$  of the same samples were also calculated using Keysight 85071E software for comparison and validation, as illustrated in Fig 6. The predicted values of  $\epsilon_r'$  and  $\epsilon_r''/\epsilon_r'$  versus operating frequencies for the four samples by using (7) and (8), respectively, are shown in Figs. 7 (a), (b) and 8. Clearly, the  $\epsilon_r'$  results were in good agreement with the measurements obtained using Agilent 85071E software.<sup>14</sup> It should be noted that the calibration planes for Figs. 5, 6 and 7 cases are refer to plane CC' and DD', which the waveguide thru-reflect-line (TRL) calibration was applied to the planes.

On the other hand, for the case of Fig. 8, the calibration is only done at plane AA' and BB' using coaxial open-short-load-thru (OSLT) technique (Keysight 85052D calibration kits). In this case, the mismatch at the surface of the sample, the waveguide and imperfections in the waveguide introduced noise in the calculations of  $\epsilon_r'$  and  $\epsilon_r''/\epsilon_r'$ . In addition, errors in the measurements can also be caused by the air gap that existed between the sample and the metal walls of the waveguide. Moreover, the flatness of the sample surfaces can also be one of the factors too. It was very challenging to get accurate results of the broadband loss tangent ( $\epsilon_r''/\epsilon_r'$ ) calculations in the case of Fig. 8 because the values of  $\epsilon_r''/\epsilon_r'$  were too small and they were very sensitive to measurement errors. In fact, the fluctuation of the random noise is larger than the values of  $\epsilon_r''/\epsilon_r'$ . Despite that, the random noise in the broadband dielectric constant measurements can be smoothed using filter techniques<sup>18</sup>.



(a) Dielectric constant,  $\epsilon'_r$

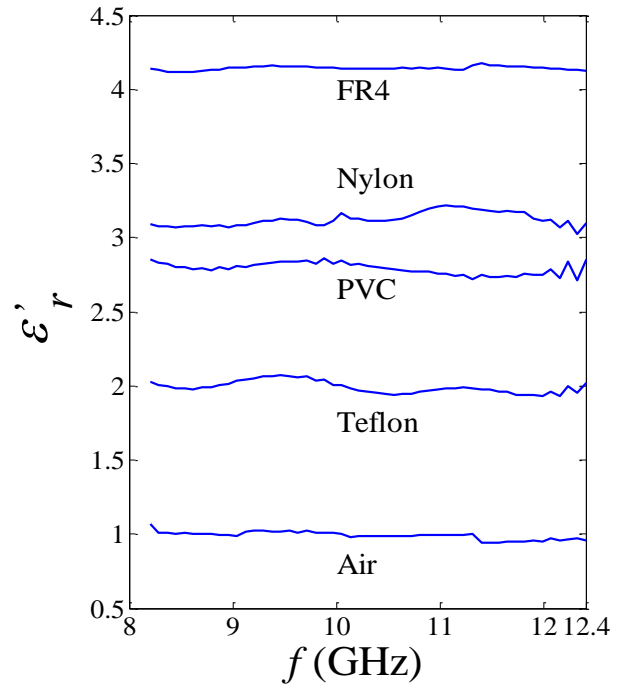
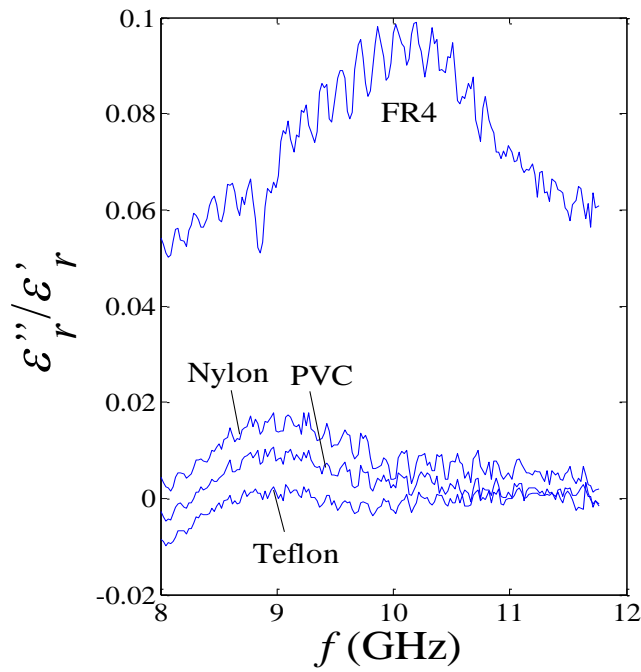
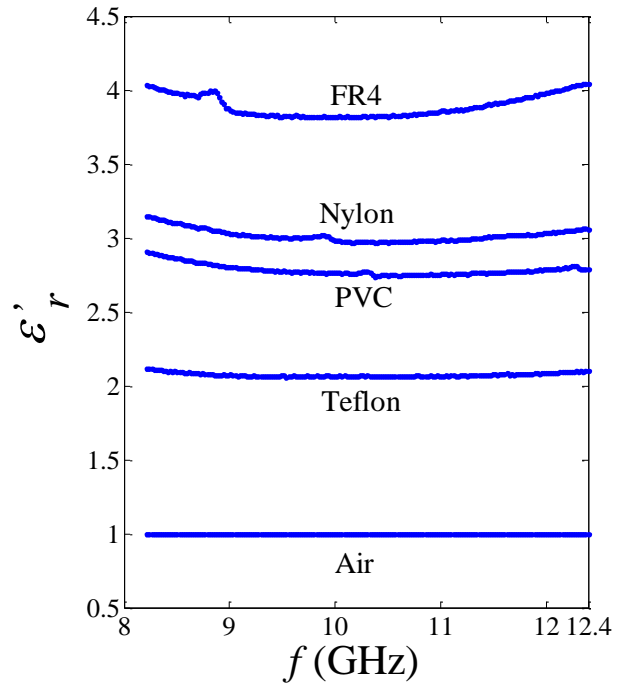


Figure 6 Comparison of measured  $\epsilon'_r$  (Keysight 85071E software with waveguide from Flann Inc.).



(b) Loss tangent ( $\epsilon''/\epsilon'_r$ )



(a) Dielectric constant,  $\epsilon'_r$

Figure 5 Comparison of (a) measured  $\epsilon'_r$  and (b) measured  $\epsilon''/\epsilon'_r$ . (NRW Method with waveguide from Flann Inc.).

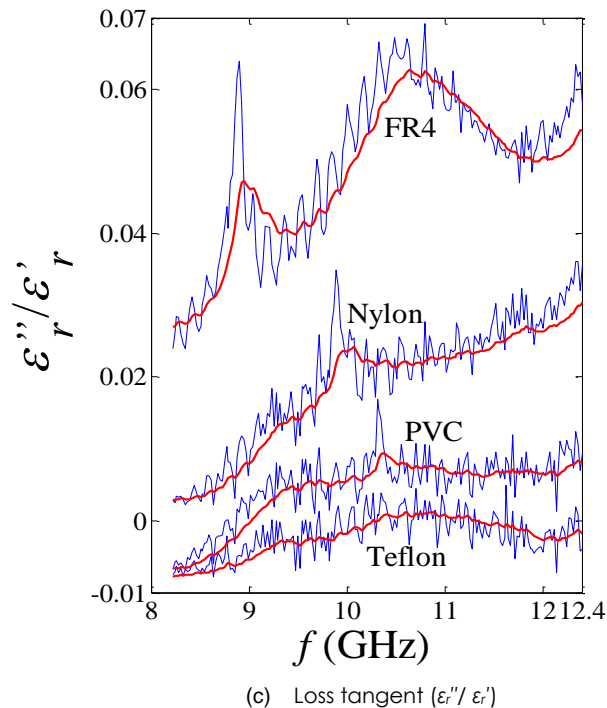


**Figure 7** Comparison of (a) measured  $\epsilon_r'$  and (b) measured  $\epsilon_r''/\epsilon_r'$  (with thru-reflect-line (TRL) calibration at plane CC' and DD'). The red solid lines are the smooth filter lines.

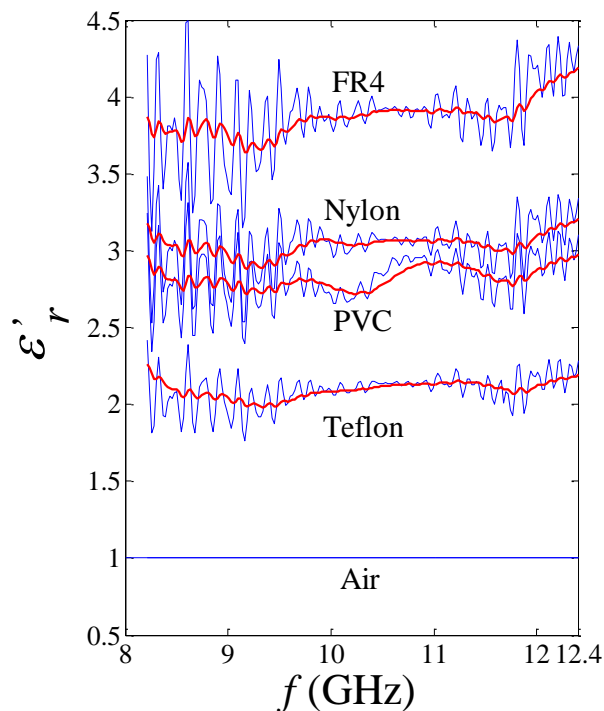


**Figure 8** Comparison of measured  $\epsilon_r'$  (with open-short-load-thru (OSLT) calibration at plane AA' and BB'). The red solid lines are the smooth filter lines.

## 5.0 CONCLUSION

In this work, equations (7) and (8) were derived to provide broadband calibration-independent and sample position-insensitive techniques for measuring the dielectric properties of low-loss materials.

## Acknowledgement

This study was supported by a Research University Grant (GUP) from Universiti Teknologi Malaysia under project number Q.J130000.2523.04H77 and the Ministry of Higher Education of Malaysia (MOHE).

## References

- [1] A. M. Nicolson, G. F. Ross. 1970. Measurement Of The Intrinsic Properties Of Materials By Time-Domain Techniques. *IEEE Trans. Instrum. Meas.* 19(4): 377-382.
- [2] W. B. Weir. 1974. Automatic Measurement Of Complex Dielectric Constant And Permeability At Microwave Frequencies. *Proc. IEEE.* 62(1): 33-36.
- [3] J. Baker-Jarvis, E. J. Vanzura, W. A. Kissick. 1990. Improved Technique For Determining Complex Permittivity With The Transmission/Reflection Method. *IEEE Trans. Microwave Theory Tech.* 38(8): 1096-1103.
- [4] A. H. Boughriet, C. Legrand, A. Chapoton. 1997. Noniterative Stable Transmission/Reflection Method For Low-Loss Material Complex Permittivity Determination. *IEEE Trans. Microwave Theory Tech.* 45(1): 52-57.
- [5] O. Luukkonen, S. I. Maslovski, S. A. Tretyakov. 2011. A Stepwise Nicolson-Ross-Weir-Based Material Parameter Extraction Method. *IEEE Antennas and Wireless Propagation Letters.* 10: 1295-1298.
- [6] K. Sarabandi, F. T. Ulaby. 1988. Technique For Measuring The Dielectric Constant Of Thin Materials. *IEEE Trans. Instrum. Meas.* 37(4): 631-636.
- [7] B. K. Chung. 2007. Dielectric Constant Measurement For Thin Material At Microwave Frequencies. *Progress in Electromagnetics Research.* 75: 239-252.
- [8] L. F. Chen, C. K. Ong, C. P. Neo, V. V. Varadan, V. K. Varadan. 2004. *Microwave Electronics (Measurement and Materials Characterization)*. U. K: John Wiley & Sons, Ltd : 175-203.
- [9] J. Sheen. 2009. Comparisons Of Microwave Dielectric Property Measurements By Transmission/Reflection Techniques And Resonance Techniques (Topical Review). *Meas. Sci. Technol.* 20: 1-12.
- [10] U. C. Hasar. 2008. A New Calibration-Independent Method For Complex Permittivity Extraction Of Solid Dielectric Material. *IEEE Microw. Wireless Compon. Lett.* 18(12): 788-790.
- [11] K. Chalapat, K. Sarvala, J. Li, G. S. Paraoanu. 2009. Wideband Reference-Plane Invariant Method For Measuring Electromagnetic Parameters Of Materials. *IEEE Trans. Microwave Theory Tech.* 57(9): 2257-2267.
- [12] Z. Caijun, J. Quanxing, J. Shenhui. 2011. Calibration-Independent And Position-Insensitive Transmission/Reflection Method For Permittivity Measurement With One Sample In Coaxial Line. *IEEE Trans. Electromagn. Compat.* 53(3): 684-689.
- [13] MathWorks. 2013. Documentation Center [Documentation Search]. Available: <http://www.mathworks.com/help/matlab/ref/unwrap.html>.
- [14] Agilent 85071 Materials Measurement Software Technical Overview. 2012. UK: Agilent Technologies Inc.
- [15] ECCOSTOCK. (R) Low Loss Dielectrics & Other Common Materials. Dielectric Materials Chart. Available:

<http://www.eccosorb.eu/sites/default/files/files/dielectric-chart.pdf>.

- [16] D. K. Ghodgaonkar, V. V. Varadan, V. K. Varadana. 1989. Free-Space Method For Measurement Of Dielectric Constants And Loss Tangents At Microwave Frequencies. *IEEE Trans. Instrum. Meas.* 37(3): 789-793.
- [17] Hitachi Chemical Co. Ltd. Low Transmission Loss Multi-Layer Material for High-Speed & High-Frequency Applications.

## Appendix

### A. Nicolson-Ross-Weir (NRW) Method

The S-parameters ( $S_{11}$  and  $S_{21}$ ) at calibrated plane  $CC'$  and  $DD'$  are measured by vector network analyzer. The  $S_{11}$  is the complex reflection coefficient of the  $d_s$  thickness of the sample at plane  $CC'$ . On the other hand, the  $S_{21}$  is the complex transmission coefficient of the  $d_s$  thickness of the sample at plane  $DD'$ .

The actual reflection coefficient,  $\Gamma$  and transmission coefficient,  $T$  of the infinite sample can be calculated using measured S-parameters<sup>1-5</sup>:

$$\Gamma = K \pm \sqrt{K^2 - 1} \quad (A1) \quad \text{and} \quad T = \frac{S_{11} + S_{21} - \Gamma}{1 - \Gamma(S_{11} + S_{21})}$$

(A2)  
where

$$K = \frac{S_{11}^2 - S_{21}^2 + 1}{2S_{11}} \quad (A3)$$

The  $|\Gamma| < 1$  condition is required in order to find the correct root value using (A1). From  $\Gamma$  and  $T$ , the relative complex permeability,  $\mu_r$  of the sample can be predicted as:

$$\mu_r = \frac{\lambda_o}{\sqrt{1 - (\lambda_o/\lambda_c)^2}} \left( \frac{1 + \Gamma}{1 - \Gamma} \right) \left[ \frac{j}{2\pi d_s} \ln \left( \frac{1}{T} \right) \right] \quad (A4)$$

And the relative complex permittivity,  $\epsilon_r$  of the sample is given as:

$$\epsilon_r = \frac{\lambda_o}{\mu_r} \left\{ \frac{1}{\lambda_c^2} - \left[ \frac{1}{2\pi d_s} \ln \left( \frac{1}{T} \right) \right]^2 \right\} \quad (A5)$$

The phase ambiguity may lead to ambiguities in retrieving the values of  $\epsilon_r$  and  $\mu_r$ . Thus, the  $\ln(1/T)$  term in (A4) and (A5) is modified as:

$$\ln \left( \frac{1}{T} \right) = \ln \left( \frac{1}{|T|} \right) + j(\phi + 2n\pi) \quad (A6)$$

where  $n$  is the integer value ( $n = 0, 1, 2, \dots$ ). From the cutoff frequency to the first resonance frequency,  $n$  is

Available:[http://www.ieee802.org/3/bj/public/nov11/iked\\_a\\_01\\_1111.pdf](http://www.ieee802.org/3/bj/public/nov11/iked_a_01_1111.pdf).

- [18] K. Y. You, Z. Abbas, M. F. A. Malek and E. M. Cheng. 2014. Non-Destructive Dielectric Measurements And Calibration For Thin Materials Using Waveguide-Coaxial Adaptors. *Measurement Science Review.* 14 (1): 16-24.

set to zero. On the other hand, from first resonance to second resonance frequency,  $n$  is set to 1.

### B. Alternative Method

For nonmagnetic sample ( $\mu_r = 1$ ), the actual reflection coefficient,  $\Gamma$  at plane  $CC'$  of an infinite dielectric sample ( $\epsilon_r = \epsilon_r' - j \epsilon_r''$ ) filled in the waveguide can be simplified as:

$$\Gamma = \frac{1 - \sqrt{\epsilon_r}}{1 + \sqrt{\epsilon_r}} \quad (B1)$$

On the other hand, the transmission coefficient,  $T$  at plane  $DD'$  can be reduced as:

$$T = \exp(-\gamma_s d_s) \quad (B2)$$

where  $\gamma_s$  is the propagation constant of the waveguide filled with  $d_s$  thickness of sample and given as:

$$\gamma_s = j \sqrt{k_o^2 (\epsilon_r' - j \epsilon_r'') - \left( \frac{\pi}{a} \right)^2} \quad (B3)$$

The measured complex value of  $S_{21}$  at plane  $DD'$  is written as<sup>1-5</sup>:

$$S_{21} = \frac{T(1 - \Gamma^2)}{1 - \Gamma^2 T^2} \quad (B4)$$

Instead (B1), (B2) and (B3) into (B4), yields

$$S_{21} = \frac{\left[ 1 - \left( \frac{1 - \sqrt{\epsilon_r}}{1 + \sqrt{\epsilon_r}} \right)^2 \right] \exp \left( -j \sqrt{k_o^2 \epsilon_r - \left( \frac{\pi}{a} \right)^2} d_s \right)}{1 - \left( \frac{1 - \sqrt{\epsilon_r}}{1 + \sqrt{\epsilon_r}} \right)^2 \exp \left( -2j \sqrt{k_o^2 \epsilon_r - \left( \frac{\pi}{a} \right)^2} d_s \right)} = 0 \quad (B5)$$

Find the value of  $\epsilon_r$  in (B5) using MATLAB's 'fsolve' command. The value of  $\epsilon_r$  is optimized in order to find a root (or zero) of (B5). For Fig. B1 case, (B5) is required to be modified as (B6).



$$S_{21} - R \frac{\left[ 1 - \left( \frac{1 - \sqrt{\epsilon_r}}{1 + \sqrt{\epsilon_r}} \right)^2 \right] \exp \left( -j \sqrt{k_o^2 \epsilon_r - \left( \frac{\pi}{a} \right)^2} d_s \right)}{1 - \left( \frac{1 - \sqrt{\epsilon_r}}{1 + \sqrt{\epsilon_r}} \right)^2 \exp \left( -2j \sqrt{k_o^2 \epsilon_r - \left( \frac{\pi}{a} \right)^2} d_s \right)} = 0 \quad (B6)$$

where  $R$  is reference plane (at plane  $DD'$ ) transformation as:

$$R = \exp \left[ j \sqrt{k_o^2 - \left( \frac{\pi}{a} \right)^2} (d - d_s) \right] \quad (B7)$$

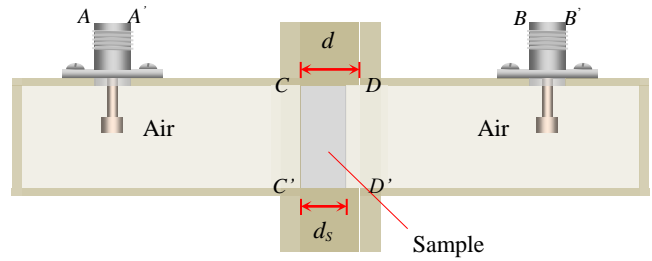


**Figure B1** Thickness of sample,  $d_s$  less than length of sample holder,  $d$  (Distance from plane  $CC'$  to plane  $DD'$ ).